

Image Captioning via Hierarchical Attention Mechanism and Policy Gradient Optimization

Shiyang Yan^{a,*}, Yuan Xie^{b,c,e}, Fangyu Wu^{d,f}, Jeremy S. Smith^d, Wenjin Lu^f,
Bailing Zhang^{b,c}

^a*School of Electronics, Electrical Engineering and Computer Science, Queen's University
Belfast, Belfast, United Kingdom*

^b*The Institute of Advanced Artificial Intelligence in Nanjing, Nanjing, China*

^c*Horizon Robotics, Beijing, China*

^d*Electrical Engineering and Electronic, University of Liverpool, Liverpool, United Kingdom*

^e*Institute of Automation, Chinese Academy of Sciences, Beijing, China*

^f*Department of Computer Science and Software Engineering, Xi'an Jiaotong-Liverpool
University, Suzhou, China*

Abstract

Automatically generating the descriptions of an image, i.e., image captioning, is an important and fundamental topic in artificial intelligence, which bridges the gap between computer vision and natural language processing. Based on the successful deep learning models, especially the CNN model and Long Short Term Memories (LSTMs) with attention mechanism, we propose a hierarchical attention model by utilizing both of the global CNN features and the local object features for more effective feature representation and reasoning in image captioning. The generative adversarial network (GAN), together with a reinforcement learning (RL) algorithm, is applied to solve the exposure bias problem in RNN-based supervised training for language problems. In addition, through the automatic measurement of the consistency between the generated caption and the image content by the discriminator in the GAN framework and

*Corresponding author

Email addresses: elyotyuan@gmail.com (Shiyang Yan), yuan.xie@ia.ac.cn (Yuan Xie), Fangyu.Wu@xjtlu.edu.cn (Fangyu Wu), J.S.Smith@liverpool.ac.uk (Jeremy S. Smith), Wenjin.Lu@xjtlu.edu.cn (Wenjin Lu), bailing.zhang@horizon.ai (Bailing Zhang)

1
2
3
4
5
6
7
8
9 RL optimization, we make the finally generated sentences more accurate and
10 natural. Comprehensive experiments show the improved performance of the hi-
11 erarchical attention mechanism and the effectiveness of our RL-based optimiza-
12 tion method. Our model achieves state-of-the-art results on several important
13 metrics in the MSCOCO dataset, using only greedy inference.
14
15
16
17

18 *Keywords:* Image captioning, Hierarchical attention mechanism, Generative
19 adversarial network, Reinforcement learning, Policy gradient
20
21

22 23 **1. Introduction**

24
25
26 2 Naturalistic description of an image is one of the primary goals of computer
27 vision, which has recently received much attention in the field of artificial intel-
28 lligence recently. It is a high-level task and much more complicated than some
29 fundamental recognition tasks, e.g., image classification [1] [2] [3] [4], image re-
30 trieval [5] [6] [7], object detection and recognition [8] [9] [10]. This requires the
31 system to comprehensively understand the content of an image and bridge the
32 gap between the image and the natural language. Automatically generating
33 image descriptions is useful in multimedia retrieval, and image understanding.
34
35
36
37
38
39
40

41 10 Some pioneering research has been carried out in generating image descrip-
42 tions [11] [12]. However, as pointed out in [13], most of these models often rely
43 on hard-coded visual concepts and sentence templates, which limits their gen-
44 eralization capability. Recently, with the rapid development of deep learning in
45 image recognition and natural language processing, the current trend of image
46 captioning approaches [14] is to follow the encoder-decoder framework, which
47 shares the similarity with that in neural machine translation [15]. Most of these
48 approaches represented the image as a single feature vector from the top layer
49 of a pre-trained convolutional neural network (CNN) and cascaded recurrent
50
51
52
53
54
55
56
57
58
59
60
61
62
63
64
65

1
2
3
4
5
6
7
8
9 19 neural network (RNN) to generate languages.

10
11 20 In fact, the tasks like image captioning and machine translation can be con-
12
13 21 sidered as a structured output problem where the task is to map the input to an
14
15 22 output that possesses its own structure, as stated in [16]. An inherent challenge
16
17 23 in these tasks is the structure of the output is closely related to the structure of
18
19 24 the input. Hence, a key problem in these tasks is alignment [16]. Take neural
20
21 25 machine translation for example, [17] trained a neural model to softly align the
22
23 26 output to the input for machine translation. Subsequent research [18] applied
24
25 27 the visual attention model to address this problem in image captioning, with
26
27 28 much improvement. The visual attention mechanism is to dynamically select
28
29 29 the relevant receptive fields in the CNN features to facilitate the image descrip-
30
31 30 tion generation, which, in other words, is to align the output words to spatial
32
33 31 regions of the source image. In this paper, we also employ the visual attention
34
35 32 mechanism for image captioning.

36
37 33 Nevertheless, natural language often consists of very meticulous descriptions,
38
39 34 which correspond to the fine-grained objects of an image. As pointed out by [19],
40
41 35 there are certain limitations of the most existing neural model-based schemes
42
43 36 due to the mere use of the global feature representation in the image level.
44
45 37 Some of the fine-grained objects might not to be recognized by only relying
46
47 38 on the global image features. In this paper, we propose to use a pre-trained
48
49 39 image detection model, i.e., Faster RCNN [10], to retrieve the fine-grained image
50
51 40 features from the top detected objects. These fine-grained object features, are
52
53 41 able to provide complementary information for the global image representation,
54
55 42 which will be proved in the experiments. In terms of the model structure, the
56
57 43 object features are also processed by a visual attention mechanism, and are

1
2
3
4
5
6
7
8
9
10
11
12
13
14
15
16
17
18
19
20
21
22
23
24
25
26
27
28
29
30
31
32
33
34
35
36
37
38
39
40
41
42
43
44
45
46
47
48
49
50
51
52
53
54
55
56
57
58
59
60
61
62
63
64
65

44 added to the original model to form a hierarchical feature representation and
45 hence it is able to generate more meticulous descriptions.

46 In addition to the improvement of the image feature representation, we also
47 consider to improve the current language model, which is widely used in neural
48 machine translation and image captioning. An issue with most of the previous
49 language model is the training framework, namely, the RNN using Maximum
50 Likelihood Estimation (MLE) to generate image descriptions. As pointed out
51 in [20], the MLE approaches suffer from the so-called exposure bias in the in-
52 ference stage: the model generates a sequence iteratively and predicts the next
53 token based on the previously predicted ones that may never be observed in
54 the training data. In image description generation, the MLE also suffers from
55 a problem that the generated languages do not correlate well with a human
56 assessment of quality [21].

57 Instead of only relying on the MLE, an alternative scheme is the generative
58 adversarial network (GAN) [22]. GAN was first proposed to generate realistic
59 images. The GAN learns generative models without explicitly defining a loss
60 function from the target distribution. Instead, GAN introduces a discriminator
61 network which tries to differentiate real samples from generated samples. The
62 whole network is trained using an adversarial training strategy. One can subse-
63 quently build a discriminator to judge how realistic are the samples generated
64 by the description generator. The role of the caption generator, in this model,
65 is similar with that of the the generator in the conditional GAN [23], which is
66 conditioned on the image features.

67 However, language generation is a discrete process. Directly providing the
68 discrete samples as inputs to the discriminator does not allow the gradients to be

1
2
3
4
5
6
7
8
9
10
11
12
13
14
15
16
17
18
19
20
21
22
23
24
25
26
27
28
29
30
31
32
33
34
35
36
37
38
39
40
41
42
43
44
45
46
47
48
49
50
51
52
53
54
55
56
57
58
59
60
61
62
63
64
65

69 back propagated through them. The reinforcement learning (RL) [24] framework
70 provides a solution to estimate the gradients of the discontinuous units. The RL
71 framework, when dealing with sequence generation, has the problem of lacking
72 the intermediate reward, as discussed in [25]. The reward value can only be
73 obtained when the whole sequence is generated. This is not suitable since what
74 we want is the long-term reward of each intermediately generated token, so the
75 whole sequence better optimized.

76 In the proposed scheme, the discriminator takes into account not only the
77 differences between the generated captions and the reference captions but also
78 the consistencies between captions and image features. Through the evaluation
79 of the discriminator, the networks can better compensate for some unrealistic
80 captions which might be generated under the MLE training. However, to deal
81 with the discreteness of language, we treat the image captioning generator as an
82 agent of RL. The feedbacks from the discriminator are considered as the rewards
83 for the generator. To update the parameters of the image description genera-
84 tor in this framework, we consider the generator as a stochastic parameterized
85 policy. We train the policy network using Policy Gradient [26], which natu-
86 rally solve the differential difficulties in conventional GAN. Also, to solve the
87 problem of lacking intermediate rewards, we borrow the idea from the famous
88 “AlphaGo” program [27] in which a Monte Carlo roll-out strategy is applied to
89 sample the expected long-term reward for an intermediate move. If we consider
90 the sequence token generation as the the action to be taken in RL, we can apply
91 a similar Monte Carlo roll-out strategy to obtain the intermediate rewards. [25]
92 has successfully applied the Monte Carlo roll-out in sequence generation. In
93 this paper, we use a similar sampling method to deal with intermediate rewards

1
2
3
4
5
6
7
8
9 94 during the process of caption generation.

10 95 To summarize, our contribution in this paper is threefold:

- 11
12
13 96 • We propose a hierarchical attention mechanism to reason on the global
14
15 97 features and the local object features for image captioning.
16
17
18 98 • The policy gradient algorithm combined with the GAN is proposed for
19
20 99 the training and optimization of the language model, with improvements
21
22 100 over MLE training scheme.
23
24
25 101 • Through comprehensive experiments, we validate the proposed algorithm
26
27 102 and comparable results with current state-of-the-art methods are achieved
28
29 103 on the MSCOCO dataset.

30
31
32 104 **2. Related Work**

33
34 105 *2.1. Deep Model-based Image Captioning*

35
36 106 Promoted by the recent success of deep learning network in image recognition
37
38 107 tasks and machine translation, the research on generating image description
39
40 108 or image captioning has made remarkable progress [28] [13] [12] [29] [14] [30].
41
42 109 As mentioned above, most of the previously proposed approaches consider the
43
44 110 image description generation as a translation process, mainly by borrowing the
45
46 111 idea of the encoder-decoder framework [31] from neural machine translation [15].
47
48 112 Generally, this paradigm considers a deep CNN model as the image encoder,
49
50 113 which maps the image into a static feature representation, and a RNN as a
51
52 114 decoder to decode this static representations to an image description. The
53
54 115 whole framework is trained using supervised learning under MLE. The generated
55
56 116 description should be grammatically correct and match the content of the image.

1
2
3
4
5
6
7
8
9
10
11
12
13
14
15
16
17
18
19
20
21
22
23
24
25
26
27
28
29
30
31
32
33
34
35
36
37
38
39
40
41
42
43
44
45
46
47
48
49
50
51
52
53
54
55
56
57
58
59
60
61
62
63
64
65

117 Specifically, Karpathy et al. [13] proposed an alignment model through a
118 multi-modal embedding layer. This model is able to align parts of a description
119 with the corresponding regions of the image, which attracts significant atten-
120 tion. Jia et al. [29] proposed a variation of LSTM, called gLSTM, for the image
121 captioning task to mainly tackle the problem of losing track of the image con-
122 tent. This model includes the semantic information along with the whole image
123 as inputs to generate captions. Donahue et al. [30] applied both of the convolu-
124 tional layers and recurrent layers to form a Long-term Recurrent Convolutional
125 Network (LRCN) for visual recognition and description.

126 Bahdanau et al. [17] pointed out that a potential problem in this approach
127 is that the model should compress all the necessary information of a source
128 sentence into a fixed-length representation. This may make it difficult for the
129 neural network to cope with long sentences. The static feature representation
130 in the encoder-decoder framework, for both of machine translation and image
131 captioning, cannot automatically retrieve relevant information from the source
132 and thus at last influence the final performance. In neural machine translation,
133 Bahdanau et al. [17] proposed a kind of soft attention mechanism for machine
134 translation, which enables the decoder to automatically focus on the relevant
135 parts of the source sentence. In computer vision, the attention mechanism
136 has long been the focus of much research [17] [32] [33] since human perception
137 does not tend to process a whole scene in its entirety at once but applies some
138 mechanisms to selectively focus on the information needed. A comprehensive
139 study for hard attention bound with reinforcement learning and soft attention
140 for the task of image captioning was published by Xu et al. [18].

141 Yao et al. [34] tackled the video captioning task through capturing global

1
2
3
4
5
6
7
8
9 142 temporal structures among video frames with a temporal attention mechanism,
10 143 which makes the model dynamically focus on the key frames that are more rel-
11 144 evant with the predicted word. Attention Models (ATT) developed by You et
12 145 al. [35] first extracted semantic concept proposals and fused them with RNNs
13 146 into hidden states and outputs. This method used K-NN, multi-label ranking to
14 147 extract semantic concepts or attributes and fused these concepts into one vector
15 148 using an attention mechanism. Similarly, Yao et al. [36] embedded attributes
16 149 with image features into a RNN with various methods to boost the image cap-
17 150 tioning performance. Recently, Chen et al. [37] proposed to combine the spatial
18 151 attention and the channel-wise attention mechanism for image captioning, with
19 152 improved results. Alternatively, Li et al. [19] proposed a global-local attention
20 153 mechanism to include local features extracted from the top detected objects
21 154 from a pre-trained object detector. Inspired by [19], we also include the local
22 155 features from top detected objects. However, we build a hierarchical model
23 156 whilst they treated local and global features equivalently.

24 157 *2.2. Policy Gradient Optimization for Image Captioning*

25 158 Another approach to boost the performance of language tasks is to com-
26 159 pensate the so-called exposure bias problem in RNN-based MLE learning. As
27 160 pointed out in [38], RNNs are trained by MLE, which essentially minimized the
28 161 KL-divergence between the distribution of target sequences and the distribution
29 162 defined by the model. This KL-divergence objective tends to favour a model
30 163 that overestimates its smoothness, which can lead to unrealistic samples [39].

31 164 In order to tackle the problems and generate more realistic image descrip-
32 165 tions, some researches directly use evaluation metrics such as BLEU [40], ME-
33 166 TEOR [41] and ROUGE [42] as the reward signal and build the model under

1
2
3
4
5
6
7
8
9 167 the RL framework. For instance, Ranzato et al. [43] is the first research us-
10 168 ing the policy gradient algorithm in a RNN-based sequence model, in which a
11 169 REINFORCE-based approach was used to calculate the sentence-level reward
12
13 170 and a Monte-Carlo technique was employed for training. Liu et al. [44] studied
14
15 171 several linear combinations of the evaluation metrics and proposed to use a lin-
16 172 ear combination of SPICE [45] and CIDEr [46] as the reward signal and apply
17
18 173 a policy gradient algorithm to optimize the model, with improved results. This
19
20 174 research used a Monte-Carlo roll-out strategy to obtain the intermediate re-
21
22 175 ward during the process of description generation. More recently, Bahdanau et
23
24 176 al. [47], instead of sentence-level reward in the training, applied the token-level
25
26 177 reward in temporal difference training for sequence generation.

27
28
29 178 As discussed previously, the GAN [22] estimates a difference measure using
30
31 179 a binary classifier, called a discriminator, to discriminate between the target
32
33 180 samples and generated samples. GANs rely on back-propagating these differ-
34
35 181 ence estimates through the generated samples to train the generator to min-
36
37 182 imize these differences. Hence, the whole network in GAN is trained in an
38
39 183 adversarial way. The GAN was originally proposed to generate naturalist im-
40
41 184 ages [22] [23] [48] [49]. Directly applying a GAN for the language problem is
42
43 185 impossible since sequences are composed of discrete elements in many applica-
44
45 186 tion areas such as machine translation and image captioning.

46
47 187 A possible solution to tackle the discreteness problem of language is to use
48
49 188 the Gumbel-Softmax approximation [50] [51]. For instance, Shetty et al. [52] use
50
51 189 a GAN to generate more realistic and accurate image descriptions with the aid
52
53 190 of Gumbel-Softmax to deal with the discontinuousness issue in language process-
54
55 191 ing. Another more general solution is to borrow an idea from the RL framework,

1
2
3
4
5
6
7
8
9
10
11
12
13
14
15
16
17
18
19
20
21
22
23
24
25
26
27
28
29
30
31
32
33
34
35
36
37
38
39
40
41
42
43
44
45
46
47
48
49
50
51
52
53
54
55
56
57
58
59
60
61
62
63
64
65

192 in which the feedback from the discriminator is considered as the reward for the
193 language generator. Dai et al. [21] built a model based on conditional GAN
194 to generate diverse and naturalistic image descriptions and paragraphs, which
195 utilizes a policy gradient for optimization. Yu et al. [25] proposed a model called
196 SeqGAN, which unified the GAN framework and RL learning problem, this has
197 recently received much attention [53] [54]. They propose a three steps training
198 strategy, which includes the pre-training the generator, pre-training the discrim-
199 inator and the final adversarial training. In this paper, inspired by the SeqGAN,
200 we propose to use a discriminator to judge the fitness of the generated image
201 descriptions with reference to the image content and apply the policy gradient
202 optimization technique [26] to train the model. Unlike the original SeqGAN, our
203 discriminator not only cares about the differences between the target language
204 and model-generated language but also considers the coherence of the language
205 with the image content.

206 **3. Approach**

207 In this section, we describe the proposed method based on two parts: the hi-
208 erarchical attention mechanism and the policy gradient optimization algorithm.

209 *3.1. Hierarchical Attention Mechanism*

210 The hierarchical attention mechanism consists of two parts: a spatial atten-
211 tion mechanism which corresponds to global CNN features and a local attention
212 mechanism which corresponds to object features.

213 The spatial attention mechanism is based on the model in [18]. Specifically,
214 the model comprises of an encoder and a decoder. We use a convolutional neural
215 network pre-trained on the ImageNet dataset [55] in order to extract a set of

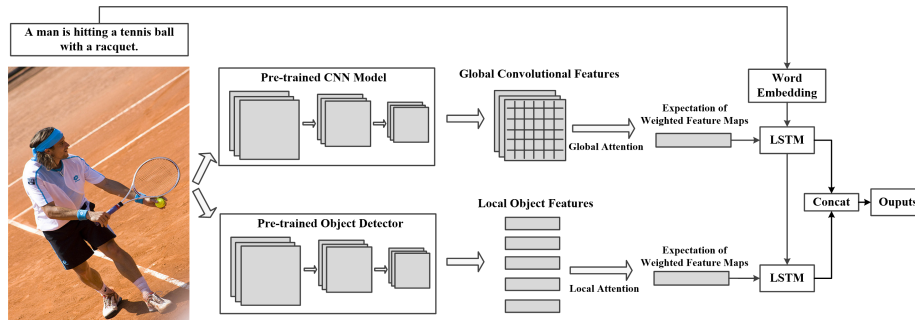


Figure 1: The hierarchical attention model structure: The CNN encoder and the object detector extracts the global and local features, respectively. These two types of features are forwarded to the LSTM models with the global and the local attention mechanisms. The outputs from the two LSTM models are concatenated and decoded to words.

convolutional features. These features, denoted as $a = \{a_1, \dots, a_L\}$, correspond to certain portions of the 2-D image. We extract convolutional features instead of fully connected ones in order to build a spatial attention mechanism since convolutional features have a spatial layout.

The Long-short Term Memory (LSTM) network, originally proposed by Hochreiter and Schmidhuber in [56], is applied as the language decoder because of its superior performance in natural language processing.

$$c_t, h_t = LSTM(z_{t-1}, c_{t-1}, h_{t-1}) \quad (1)$$

In Equation 1, c_t and h_t are the memory cells and hidden states of the LSTM, respectively. z_t is the context vector, which can be processed by the soft attention mechanism and is able to capture visual information associated with a certain input location. The soft attention mechanism has to automatically allocate adaptive weights for the image locations to facilitate the task at hand.

$$a = \text{Average_Pooling}(a_i), i = 1 \dots L \quad (2a)$$

$$e_{ti} = \text{MLP}(a, h_{t-1}) \quad (2b)$$

$$\alpha_{ti} = \frac{\exp(e_{ti})}{\sum_{k=1}^L \exp(e_{tk})} \quad (2c)$$

$$z_t = \sum_{i=1}^L \alpha_{ti} a_i \quad (2d)$$

228 where $a_i \in \{a_1, \dots, a_L\}$. The first and second equations of Equation 2 map
 229 the image features from each location, along with information from the hidden
 230 state, into an adaptive weight, which indicates the importance of each image
 231 location for the recognition. Then, we normalize the adaptive weights into a
 232 probability value in the range of 0 and 1 using the Softmax function. Once these
 233 weights (summed to 1) are computed, we element-wisely multiply the weights
 234 vector α_t with image feature vector a and sum them to the context vector z_t ,
 235 which can be expressed as in the last equation of Equation 2. This can be seen
 236 as the expectation of weighted features maps. Then the context vector z_t is
 237 forwarded to the LSTM network to generate captions, as described in Equation
 238 1. This soft attention mechanism is able to adaptively select the relevant visual
 239 parts of the given image features and thus facilitate the recognition.

240 The local attention mechanism is formulated using object features and an-
 241 other LSTM model. We use a pre-trained object detector to retrieve the top N
 242 detected object features, which are denoted as $d = \{d_1, \dots, d_N\}$. We then use
 243 another LSTM model with soft attention to allocate adaptive weights to each
 244 of these features.

$$z_t^d = \text{Concat}\left(\sum_{i=1}^N \alpha_{ti}^d d_i, h_{t-1}\right) \quad (3)$$

Equation 3 demonstrates that the context vector for local attention model catching information from both the local features and the global attention mechanism, where *Concat* indicates the concatenation operation of the features. This context vector is then forwarded to a second LSTM model.

The two LSTM models, denoted as $LSTM^G$ for the global features and $LSTM^L$ for the local features are jointly trained to map the hierarchical feature representation with language. $LSTM^L$ is at a higher level, which can be used to decode the hidden states for the final outputs. However, the gradient vanishing problem cannot be avoided if we only use the hidden states from $LSTM^L$ to decode information. Inspired by [3] in which a shortcut in network connections is applied to solve the gradient vanishing problem, we concatenate the hidden states from $LSTM^G$ and $LSTM^L$ to decode and map the hidden states to language vectors, which can be seen in Equation 4.

$$h_t^{output} = Concat(h_t, h_t^d) \quad (4a)$$

$$logits = W_p h_t^{output} \quad (4b)$$

$$P(s_t|I, s_0, s_1, s_2, \dots, s_{t-1}) = Softmax(logits) \quad (4c)$$

In MLE training, if the length of a sentence is T , the loss function can be formulated as in Equation 5, which is the sum of the log likelihood of each word.

$$Loss = \sum_{i=0}^T \log(p(s_t|I, s_0, s_1, s_2, \dots, s_i)) \quad (5)$$

3.2. Policy Gradient Optimization

In addition to only using the MLE to train the image caption generator, to alleviate the previously discussed exposure bias problem in RNN-based MLE

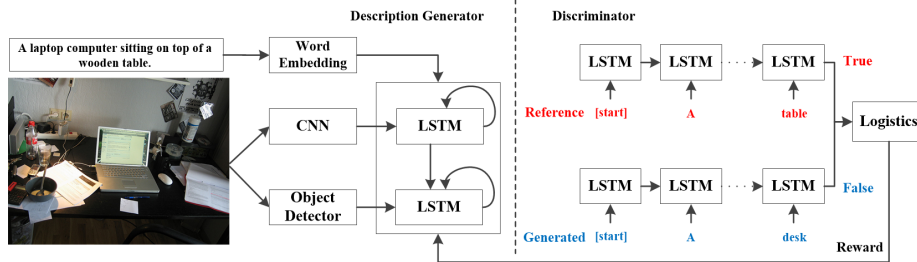


Figure 2: Policy Gradient optimization with a discriminator to evaluate the similarity between the generated sentence and the reference sentence.

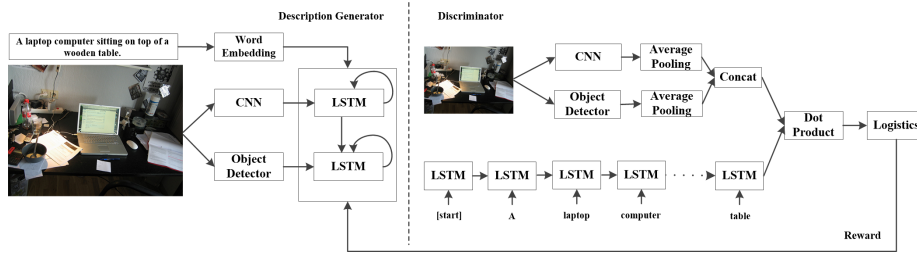


Figure 3: Policy Gradient optimization with a discriminator to evaluate the coherence between the generated sentence and the image contents.

263 training as discussed previously, we also apply a policy gradient optimization
 264 algorithm in the RL framework to increase the quality of the generated descrip-
 265 tions.

266 We feed both of the generated descriptions and the reference descriptions to
 267 the discriminator. The level of coherence of the descriptions and image content
 268 is calculated by the dot product, which is forwarded to the discriminator, as
 269 described in Fig. 3. This operation is to consider the coherence between certain
 270 captions (sequences) and corresponding image features, which is able to make
 271 the generated captions more realistic and naturalistic. The reference sequences
 272 are labeled as true whilst the generated sequences are labeled as false during
 273 the training of the discriminator. The model is also a LSTM network with

1
2
3
4
5
6
7
8
9
274 Softmax Cross Entropy loss. Hence, the discriminator outputs the probabilities
10
275 of a sample being true. These probabilities, are then considered as the reward
11
12
276 signal in the RL framework, to be utilized in the Policy Gradient algorithm for
13
14
277 updating the parameters of the image caption generator.

15
16
278 Following [26], the objective of the policy network $G_\theta(y_t|y_{1:t-1})$ (the image
17
18
279 caption generator), is to generate a sequence from the start state S_0 to maximize
19
20
280 its expected long-term reward as described by Equation 6:

$$J(\theta) = E[R_T|s_0, \theta] = \sum_{y_1 \in Y} G_\theta(y_1|s_0) \cdot Q_{D_\theta}^{G_\theta}(s_0, y_1) \quad (6)$$

21
22
23
24
25
26
27 where R_T is the reward for a complete sequence. $Q_{D_\theta}^{G_\theta}(s, y)$ is the action-value
28
282 function of a language sequence, which is defined as the expected accumulative
29
30
283 reward starting from state s , taking a certain action, and then following policy
31
32
284 G_θ .

33
34
285 The action-value function is estimated using the REINFORCE algorithm [57]
35
36
286 and considers the probability of being real generated by the discriminator as a
37
38
287 reward, which can be defined as in Equation 7.

$$Q_{D_\theta}^{G_\theta}(a = y_T, s = Y_{1:T-1}) = D_\theta(Y_{1:T}) \quad (7)$$

39
40
41
42
43
44
288 As can be seen in Equation 7, the discriminator only provides a reward for
45
46
289 a complete sequence. We should not only care about the reward for a complete
47
48
290 tokens but also the long-term reward for the future time-steps since the long-
49
50
291 term reward is what we actually want. Similar to the game of Go [27] in which
51
52
292 the agent sometimes give up an immediate interest but cares about the final
53
54
293 victory, we apply a similar Monte Carlo roll-out strategy for an intermediate
55
56
294 state, i.e., an unfinished sequence. We represent an N-time Monte Carlo search
57
58

1
2
3
4
5
6
7
8
9 as in Equation 8.

$$Y_{t+1:T}^1, \dots, Y_{t+1:T}^n, \dots, Y_{t+1:T}^N = MC^{G_\theta}(Y_{1:t}; N) \quad (8)$$

$$MC \sim \text{Multinomial}(\text{logits})$$

10
11
12
13
14
15
16 where $Y_{1:t}$ is the generated sequence tokens and $Y_{t+1:T}^n$ is the Monte Carlo
17
18 sampled based on a roll-out policy, which, in our case, is set as the same as the
19
20 image caption generator for convenience. In reality, we can use any policy to
21
22 perform the roll-out operation. *logits* is the output of the LSTM decoder. MC
23
24 is defined as a sampling procedure from a Multinomial distribution.

25
26 If there is no intermediate reward, the Monte Carlo roll-out strategy can
27
28 sample the future possible tokens N times and average these rewards to achieve
29
30 the goal of reward estimation, which is described in Equation 9.

$$Q_{D_\theta}^{G_\theta}(a = y_t, s = Y_{1:t-1}) = \begin{cases} \frac{1}{N} \sum_{n=1}^N D_\theta(Y_{1:T}^n, Y_{1:T}^n \in MC^{G_\theta}(Y_{1:t}; N)), & \text{for } t < T \\ D_\theta(Y_{1:T}), & \text{for } t = T \end{cases} \quad (9)$$

31
32
33
34
35
36
37
38
39
40 The Monte Carlo roll-out strategy can be better visualized in Fig. 4.

41
42 Once the reward value from the discriminator is obtained, it is ready to
43
44 update the generator. The goal is to maximize the average reward starting
45
46 from the initial state as defined in Equation 10.

$$J(\theta) = \frac{1}{N} \sum_{i=1}^N V_\theta(s_0 | X_i, Y_i) \quad (10)$$

47
48
49
50
51
52 where N is the number of samples used for training. We can use the Policy
53
54 Gradient theorem from [26] and write the gradient of the objective function
55
56
57
58
59
60
61
62
63
64
65

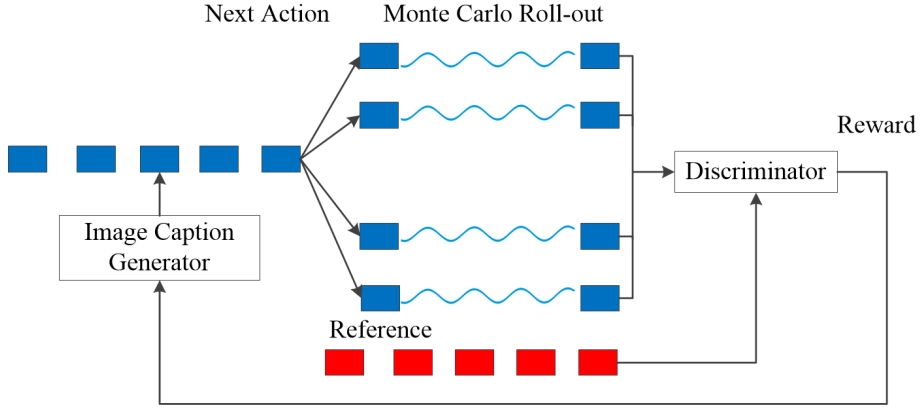


Figure 4: Monte Carlo roll-out: We use Monte Carlo sampling to sample tokens in the future time steps and average them to obtain the intermediate rewards so as to optimize the token generated at each time step.

(reward signal) as in Equation 11.

$$\nabla_{\theta} J(\theta) = E_{Y_{1:t-1} \sim G_{\theta}} \left[\sum_{y_t \in Y} \nabla G_{\theta}(y_t | Y_{1:t-1}) \cdot Q_{D_{\theta}}^{G_{\theta}}(Y_{1:t-1}, y_t) \right] \quad (11)$$

Since the expectation can be approximated by sampling, we can now update the parameters of the image caption generator using Equation 12.

$$\theta \leftarrow \theta + \alpha_h \nabla_{\theta} J(\theta) \quad (12)$$

In practice, we can use advanced gradient algorithms such as RMSprop [58] and Adam [59] in training the caption generator.

The image caption generator and discriminator are adversarially trained in the framework of GAN [22]. In GAN [23], the discriminator can pass the gradient directly to the generator. Due to the discreteness of the sequence generation, we apply RL to estimate the gradient of the generator in our model.

Specifically, the training strategy is described in Algorithm 1. We initially

1
2
3
4
5
6
7
8
9 320 pre-train the image caption generator using MLE. In practice, this is equivalent
10 321 to the Cross Entropy loss [60]. Hence, we can set the pre-training step the
11 322 same as in [18]. The trained model is used to generate some captions which
12 323 are set as fake samples, which, along with the reference captions, are fed into
13 324 the discriminator for training. Similarly, the discriminator is also pre-trained
14 325 for certain steps. The next steps are the adversarial training steps, in which
15 326 the image caption generator and discriminator are trained alternatively until
16 327 convergence of the networks.

17
18 328 In addition to the sentence comparison scheme introduced previously, and
19 329 shown in Fig. 2, we also employ a scheme to evaluate the coherence between
20 330 the generated captions and the image content. Specifically, both of the global
21 331 features and local object features are processed by average pooling in order to
22 332 obtain fixed-size feature representation, denoted as V_i . The captions, similar
23 333 to the sentence comparison scheme, are also encoded into a fixed-size vector,
24 334 using a LSTM model, denoted as V_w . The two vectors V_i and V_w are then
25 335 dot producted and forwarded to logistic function to obtain the reward for RL
26 336 training, which can be seen in Fig. 3.

337 4. Experimental Validation

338 4.1. Dataset Introduction

339 We conduct our experiments using the MSCOCO dataset [61]. To be consis-
340 tent with the previous researches, we use the MSCOCO 2014 released version,
341 which includes 123,000 images. The dataset contains 82,783 images in the train-
342 ing set, 40,504 images in the validation set and 40,775 images in the test set. As
343 the ground-truth for the MSCOCO test set is not available, the validation set is

Algorithm 1 Image Caption Generation by Adversarial Training and Reinforcement Learning

Input: Image Caption Generator G_θ ; Discriminator D_θ .

Pre-training G_θ using MLE by 10 epoches.

Generating negative samples using pre-trained G_θ to train D_θ .

Pre-training D_θ by 2500 steps.

repeat

for update-generator for 1 step **do**

 Generate a sequence $Y_{1:T} = (y_1, \dots, y_T)$.

for $t = 1$ to T **do**

 Compute the intermediate reward $Q(t)$ by Monte Carlo roll-out.

end for

 Update the parameters θ using Policy Gradient.

end for

for update-discriminator for 1 step or 5 steps **do**

 Training discriminator D_θ using reference sequence (True) and generated sequence (Fake) using current generator.

end for

until Convergence

Table 1: Parameter Settings of the Hierarchical Image Encoder

Global Image Decoder	Global Image Features Dimension	Faster RCNN model	Local Image Features Dimension
Residual-152	49×2048	VGG16	30×4096

Table 2: Parameter Settings of the Language Decoder

Word Embedding Dimension	$LSTM^G$ Dimension	$LSTM^L$ Dimension	Maximum Sequence Length (Training)	Maximum Sequence Length (Inference)
512	512	512	20	30

21 further splitted into a validation subset for model selection and a test subset for
 22 local experiments. This is the ‘‘Karpathy’’ split [13]. It utilizes the whole 82,783
 23 training set images for training, and selects 5,000 images for validation and 5,000
 24 images for testing from the official validation set. The standard evaluation pro-
 25 tocol contains BLEU [40], METEOR [41], CIDEr [46] and ROUGE-L [42].
 26
 27
 28
 29
 30

31 BLEU is the most popular metric for the performance evaluation in machine
 32 translation. The metric is only based on the n-gram statistics. The BLEU-
 33 1, BLEU-2, BLEU-3 and BLEU-4 measure the performance of the 1, 2, 3,
 34 4-gram, respectively. METEOR is based on the harmonic mean of unigram
 35 precision and recall, and seeks correlation at the corpus level. CIDEr can be
 36 used to evaluate the generated sentences with human consensus. ROUGE-L
 37 measures the common maximum-length subsequence for the target sentence
 38 and the generated sentence.
 39
 40
 41
 42
 43
 44
 45

357 *4.2. Implementation Details*

358 The whole pipeline of the algorithm and implementation procedure are pre-

Table 3: Parameter Settings of Training

MLE Pre-training	Batch Size	Learning Rate of MLE	Optimizer	Discriminator Pre-training	Learning Rate of Policy Gradient
10 epochs	32	0.001	Adam	2500 iterations	0.0001

Algorithm 2 The whole pipeline of the proposed method

Pre-train the Faster R-CNN on the MSCOCO dataset.

Extract features via Residual-152 and the pre-trained Faster R-CNN.

Language pre-processing.

MLE pre-training.

Perform Algorithm 1.

359 sented in Algorithm 2. For all the images in the COCO dataset, we obtain global
360 convolutional features (from the layer “res5c”) using a pre-trained Residual-152
361 network [3] on the platform of Caffe [62], with a dimensionality of 49×2048 .
362 We also retrieve local object features using a Faster RCNN [10] object detec-
363 tion network pre-trained on the MSCOCO dataset. Specifically, we obtain the
364 top K detected object features from the layer of “FC6” layer of the VGG16
365 model [2] used in Faster RCNN, with dimensionality of $K \times 4096$. We build
366 the hierarchical attention mechanism and policy gradient optimization on the
367 TensorFlow platform [63].

368 4.2.1. Training the Faster RCNN on the MSCOCO dataset

369 In order to obtain better local object features, we train the Faster RCNN
370 model on MSCOCO object detection dataset. The model is first pre-trained
371 on the ImageNet object detection dataset [55]. The MSCOCO object detection
372 dataset shares the same images with the image caption task. Consequently, we
373 keep the same splits with the image caption dataset for training. The training
374 process on the MSCOCO dataset is almost the same with the pre-training on
375 ImageNet. The initial learning rate is set to 0.001. The momentum of the
376 stochastic gradient descent is set to 0.9 and the weight decay is set to 0.0005.

1
2
3
4
5
6
7
8
9
10
11
12
13
14
15
16
17
18
19
20
21
22
23
24
25
26
27
28
29
30
31
32
33
34
35
36
37
38
39
40
41
42
43
44
45
46
47
48
49
50
51
52
53
54
55
56
57
58
59
60
61
62
63
64
65

377 *4.2.2. Language Pre-processing*

378 To pre-process the language, the special symbols such as ‘.’, ‘,’ , ‘(’, ‘)’ and
379 ‘-’ are replaced with blank spaces whilst ‘&’ is replaced with ‘and’. Since we
380 set the maximum length of the descriptions as 20 words, we delete the caption
381 references from the original dataset which are longer than 20. For the vocabulary
382 establishment, following the open-source code of [13], we include words that
383 occurs more than 5 times in the vocabulary. We map the symbol ‘NULL’ to 0,
384 ‘START’ to 1 and ‘END’ to 2.

385 *4.2.3. Training Details of the Model*

386 Following the open-source code of [13], at training time, we set the maximum
387 length of the input sequence to 20 words. During the testing time, alternatively,
388 we set maximum length of a generated symbols as 30 words. During the training
389 of the proposed model, we add a trainable word embedding layer from Google’s
390 TensorFlow platform [63]. All the experiments are conducted on a server em-
391 bedded with NVIDIA TITAN X GPU and installed with the Ubuntu 14.04
392 operating system. We summarise the parameters of the model and training in
393 Table 1, Table 2 and Table 3. Our code is publicly available at ¹.

394 *4.3. Results*

395 *4.3.1. Quantitative Evaluation*

396 In this section, a comprehensive quantitative evaluation is conducted using
397 different experimental settings on the MSCOCO dataset.

¹<https://github.com/Shiyang-Yan/image-captioning-with-hierarchical-attention-and-policy-gradient-optimisation>

1
2
3
4
5
6
7
8
9
10
11
12
13
14
15
16
17
18
19
20
21
22
23
24
25
26
27
28
29
30
31
32
33
34
35
36
37
38
39
40
41
42
43
44
45
46
47
48
49
50
51
52
53
54
55
56
57
58
59
60
61
62
63
64
65

398 *Comparison between the global attention, the local attention and the hierarchi-*
399 *cal attention model.* We first obtain the results using only the global attention
400 model, which is similar to the soft attention model in [18]. Since we use advanced
401 CNN features from the Residual-152 model, the results of BLEU, METEOR,
402 CIDEr and ROUGE-L are all satisfactory, and are listed in Table 4. Then
403 only the local attention model using the detected object features from a Faster
404 RCNN detector is tested, with results which are much lower than those for the
405 global attention model as listed in Table 4. One of the possible reasons is that
406 the Faster RCNN only uses the VGG16 model, which is not as powerful as the
407 Residual-152 network. Another reason is that the local object features, despite
408 the capability to provide complementary information to the global attention
409 model, can sometimes miss many important features. Finally, we test our pro-
410 posed hierarchical attention model under MLE training, which utilizes both of
411 the global and local attention for image captioning. The results improve the
412 baseline significantly, which can be seen in Table 4. Specifically, all of the seven
413 evaluation metrics are improved using our hierarchical attention model.

414 *The determination of the number of top detected objects.* To determine the best
415 number k for the top detected objects in the local attention model, we perform
416 an ablation study. We extract the 10, 20 and 30 top detected object features
417 and test them using the hierarchical attention model. The results can be seen
418 in Table 5. With the increase of the number k from 10 to 30, the performance
419 increases accordingly. Although the maximum length of our generated sentences
420 is set as 30, not every word represents an object. Also, intuitively, there are a
421 maximum 30 objects within an image. Hence, in the following experiments, we
422 use the 30 top detected object features for the local attention model.

Table 4: Comparison of image captioning using different attention mechanism results on the MSCOCO dataset

Methods	BLEU-1	BLEU-2	BLEU-3	BLEU-4	METEOR	CIDEr	ROUGE-L
Soft Attention [18]	70.7	49.2	34.4	24.3	23.90	-	-
Global Attention	70.121	50.304	35.434	25.111	23.658	84.701	54.308
Local Attention	64.059	42.359	28.089	19.033	20.203	56.898	49.861
Hierarchical Attention	72.611	52.769	37.802	27.243	24.731	88.140	56.048

Table 5: Comparison of image captioning results on the MSCOCO dataset with different numbers of objects

Methods	BLEU-1	BLEU-2	BLEU-3	BLEU-4	METEOR	CIDEr	ROUGE-L
Hierarchical Attention with 10 Objects for Local Attention	70.601	50.423	36.643	25.389	24.633	87.316	55.241
Hierarchical Attention with 20 Objects for Local Attention	72.159	52.498	37.552	26.918	24.725	88.639	55.825
Hierarchical Attention with 30 Objects for Local Attention	72.611	52.769	37.802	27.243	24.731	88.140	56.048

Table 6: Comparison of image captioning results on the MSCOCO dataset with different settings for policy gradient (PG) optimization

Methods	BLEU-1	BLEU-2	BLEU-3	BLEU-4	METEOR	CIDEr	ROUGE-L
MLE training only	72.611	52.769	37.802	27.243	24.731	88.140	56.048
PG with 2500 steps for pre-training D followed by 1 D and 1 G step	72.450	52.845	38.141	27.551	24.543	87.416	55.876
PG with 2500 steps for pre-training D followed by 5 D and 1 G step	72.104	52.739	38.122	27.602	24.928	89.072	56.063

423 *The performance of Policy Gradient with reward only from language compar-*
 424 *ison.* Next we start the reinforcement learning steps. We first train the dis-
 425 criminators which only compares the similarity between the reference sentence
 426 and the generated sentence. Specifically, we follow the model defined in Fig.
 427 2. The discriminator is first trained in 2500 steps, which we find sufficient for
 428 the discriminator to converge. The loss curve of the image caption generator
 429 is shown in Fig. 5. After 2500 steps pre-training the discriminator, the loss of
 430 the image caption generator starts to decline, which validates that the policy
 431 gradient starts to work. Then we further train the generator and discriminator

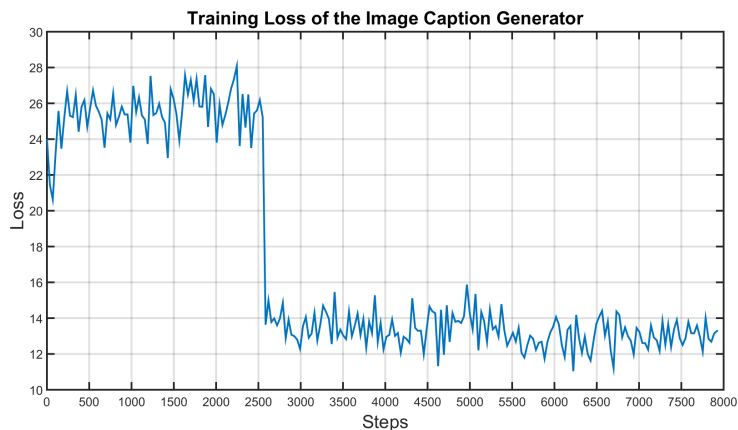


Figure 5: The loss curve of the image caption generator during reinforcement learning steps: before 2500 iterations, we pre-train the discriminator. Starting from the 2500 iterations, we start the adversarial training of the generator and discriminator. The loss value starts to decrease starting from 2500 iterations as the parameters of the generator begins to be updated.

432 adversarially for another 1 epoch, and report the results in Table 6. We also
 433 experimented with two different settings in the adversarial training steps. The
 434 first setting is to train 1 step for the discriminator, followed by another step for
 435 the generator. Another setting is to train the discriminator for 5 steps, followed
 436 by 1 step training for the generator. We find the final results of the two setting
 437 are similar, which all slightly improve the MLE training baseline. The reason for
 438 the improvement is because the reinforcement learning solves the exposure bias
 439 problem during MLE training. However, this scheme lacks the measurement
 440 of the similarity between the generated descriptions and the image contents,
 441 which prevents the image caption generator from generating more naturalistic
 442 and diverse descriptions.

443 *The performance of Policy Gradient with reward from the measurement of coher-*
 444 *ence between language and image content.* To train the image caption generator

Table 7: Comparison of image captioning results on the MSCOCO dataset for policy gradient (PG) optimization with discriminator for evaluation of the coherence between language and image content.

Methods	BLEU-1	BLEU-2	BLEU-3	BLEU-4	METEOR	CIDEr	ROUGE-L
MLE training only	72.611	52.769	37.802	27.243	24.731	88.140	56.048
Global Attention	70.121	50.304	35.434	25.111	23.658	84.701	54.308
PG with similarity of global features (1 D and 1 G step)	72.250	52.290	37.099	26.331	23.815	84.516	55.238
PG with similarity of global features (5 D and 1 G step)	72.234	52.120	36.887	26.065	23.957	84.224	55.244
PG with similarity of global-local features (1 D and 1 G step)	73.036	53.688	39.069	28.551	25.324	92.449	56.539

to generate more naturalistic and diverse descriptions, we further test the model defined in Fig. 2. First we only extract the global features and perform average pooling, resulting with a feature dimension of 2048. We then use the dot product to measure these image features and language embedding features by a discriminator, which can be considered as the reward within the reinforcement learning framework. The experimental results from this model can be seen in Table 7.

However, the results from all of the seven metrics are even lower than the MLE training baseline. One possible reason, is the measurement of discriminator which only uses the global features, which is not consistent with the hierarchical attention model in the generator side. As can be seen from the Table 7, the results from this model are similar to that of global attention model, since the reward signal from the discriminator tends to force the generator to produce sentences that only matches the global features.

We further build a model exactly like in the one defined in Fig. 3. This model includes both of the global image features and the local object features, and thus guarantees that the discriminator and the generator are utilizing the same information source. The final results can be seen in Table 7, which outperform

Table 8: Comparison of image captioning results on the MSCOCO dataset with previous methods.

Methods	BLEU-1	BLEU-2	BLEU-3	BLEU-4	METEOR	CIDEr	ROUGE-L
Google NIC [14]	66.6	46.1	32.9	24.6	-	-	-
m-RNN [28]	67	49	35	25	-	-	-
BRNN [13]	64.2	45.1	30.4	20.3	-	-	-
MSR/CMU [64]	-	-	-	19.0	20.4	-	-
Spatial Attention [18]	71.8	50.4	35.7	25.0	23.0	-	-
gLSTM [29]	67.0	49.1	35.8	26.4	22.7	81.3	-
GLA [19]	56.8	37.2	23.2	14.6	16.6	36.2	41.9
MIXER [43]	-	-	-	29.0	-	-	-
Conv Image Caption [65]	71.1	53.8	39.4	28.7	24.4	91.2	52.2
SCA-CNN-ResNet [37]	71.9	54.8	41.1	31.1	25.0	-	-
Semantic Attention [35]	70.9	53.7	40.2	30.4	24.3	-	-
DCC [66]	64.4	-	-	-	21.0	-	-
RL with G-GAN [21]	-	-	30.5	29.7	22.4	79.5	47.5
RL with Embedding Reward [67]	71.3	53.9	40.3	30.4	25.1	93.7	52.5
Self-Critical (CIDEr) [68]	-	-	-	31.9	25.5	106.3	54.3
Ours	73.036	53.688	39.069	28.551	25.324	92.449	56.539

all of other experimental settings.

To prove the effectiveness of the proposed method, we compare our final results on the “Karpathy” test split with previously published results, which is shown in Table 8. We list most of the published results on the “Karpathy” split, which are grouped into three categories. The first category corresponds to various methods without external information and reinforcement learning. The best of them (SCA-CNN-ResNet) is the spatial and channel-wise attention model [37] in which both the spatial and channel-wise attention mechanisms are utilized for image captioning. The methods in the second group use extra information during the training of the model. For instance, Semantic Attention [35] utilizes rich extra data from social media to train the visual attribute predictor.

1
2
3
4
5
6
7
8
9 474 Deep Compositional Captioning (DCC) [66] generates extra data to prove its
10 475 unique transfer capability. The third group corresponds to the reinforcement
11 476 learning technique. RL with G-GAN [21] applies conditional GAN and policy
12 477 gradient to generate image descriptions. Although their results on the eval-
13 478 uation metrics are not improved, they prove that the generated captions are
14 479 more diverse and naturalistic. Embedding Reward [67] applies a policy network
15 480 to generate captions and a value network to evaluate the reward. Additionally,
16 481 they also apply advanced inference method called lookahead inference and beam
17 482 search during testing. They achieve the current state-of-the-art results on the
18 483 “Karpathy” split. Although we do not use any external knowledge and any
19 484 advanced inference technique (including beam search, we use greedy search in
20 485 all of our experiments), we achieve similar results to the current state-of-the-art
21 486 methods (Embedding Reward [67], SCA-CNN-ResNet [37] and self-critical [68]),
22 487 with state-of-the-art results on two important metrics: BLEU-1 and ROUGE-L
23 488 and lead other methods significantly.

24 489 *4.3.2. Qualitative Evaluation*

25 490 In addition to the quantitative evaluation using the standard metrics, we
26 491 qualitatively evaluate the proposed model by visualization. Firstly, we plot
27 492 some global attention maps corresponding to each generated words as shown in
28 493 Fig. 6. It is obvious in the figure that the attentive regions normally correspond
29 494 with the semantic meaning of the generated word in each time step. Then we
30 495 choose some examples to visualize the local attention weights on the detected
31 496 objects, which are shown in Fig. 7. We only retrieve the top 10 detected
32 497 objects and corresponding attentive weights obtained from the local attention
33 498 mechanism because of limited space in the figure. The detector can detect

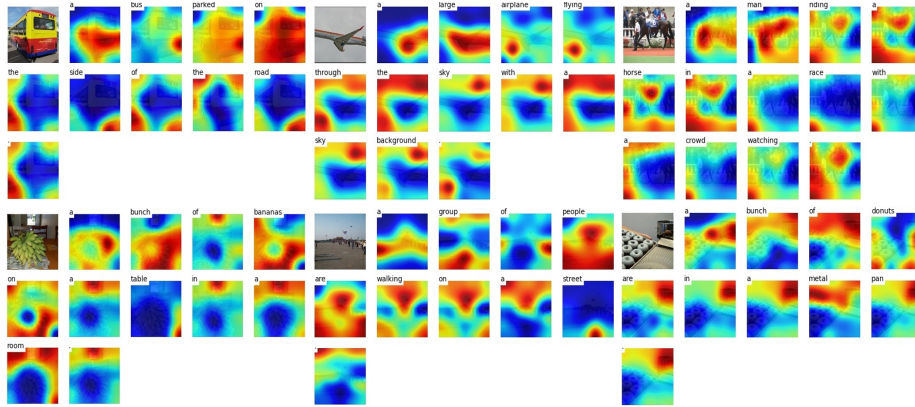


Figure 6: Visualization of the global attention maps and generated captions. The red color indicates the importance of each region of the image.

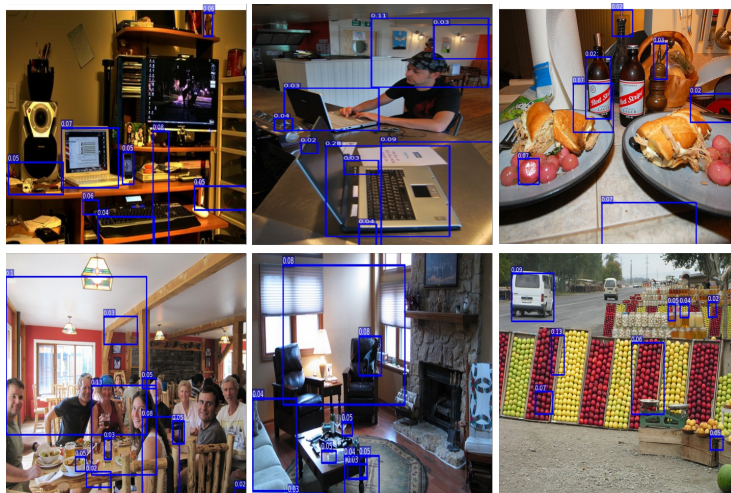


Figure 7: Visualization of the attentive weights on the top 10 detected objects, the blue boxes indicate the detected objects whilst the labels show the attentive weights of the local attention model.

1
2
3
4
5
6
7
8
9
10
11
12
13
14
15
16
17
18
19
20
21
22
23
24
25
26
27
28
29
30
31
32
33
34
35
36
37
38
39
40
41
42
43
44
45
46
47
48
49
50
51
52
53
54
55
56
57
58
59
60
61
62
63
64
65

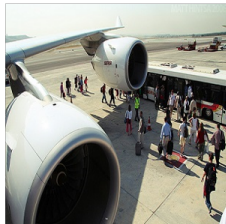


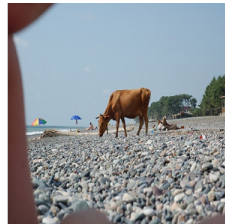


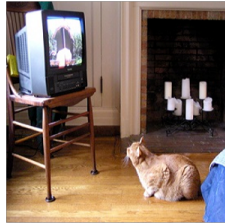
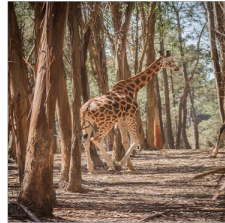
			
Reference: A group of people standing next to a bus under an airplane.	Reference: A yellow and red bus parked in a parking lot with other busses.	Reference: A little boy sitting in front of a hot dog covered in ketchup.	Reference: The lone adult cow walks on rocks near the beach.
MLE: A large airplane is parked on the runway.	MLE: A yellow bus is parked on the side of the road.	MLE: A little girl is eating a hot dog.	MLE: A cow is walking down the street in the sand.
Ours: A large airplane is parked on the runway with people walking around.	Ours: A yellow and red bus parked in a parking lot.	Ours: A young boy is eating a hot dog.	Ours: A cow is standing on the beach next to body of water.
			
Reference: A baseball player swinging a baseball bat during a game.	Reference: Six cows standing and laying on the beach.	Reference: A fat cat in the living room watching the tv.	Reference: A giraffe is walking through the forest with tall trees.
MLE: A baseball player is preparing to swing at a pitch.	MLE: A group of cows standing on top of a snow covered field.	MLE: A cat is sitting in a living room with a television.	MLE: A giraffe is standing in the woods with trees in the background.
Ours: A baseball player is swinging a bat at a ball..	Ours: A group of cows standing on top of a sandy beach.	Ours: A cat sitting on the floor watching a television.	Ours: A giraffe standing next to a tree in a forest.

Figure 8: The visualisation of some captioning results.

1
2
3
4
5
6
7
8
9 499 some fine-grained objects, which provide complementary information for the
10 global attention mechanism. At last, we show some of the generated sentences
11 500 using different methods. Specifically, we show the ground-truth sentences, de-
12 501 scriptions generated by the MLE training-based model and by the proposed
13 502 model as shown in Fig. 8. The text in blue are the sentences generated by the
14 503 proposed model, which are more accurate and naturalist than the MLE-based
15 504 model, which are shown in green. Specially, the proposed model show supe-
16 505 rior performance in finding the fine-grained properties of the image since the
17 506 RL model automatically measure the coherence of the sentences and the image
18 507 content.
19 508 content.

509 **5. Conclusion**

510 This paper targets the image captioning task, which is a fundamental prob-
511 lem in artificial intelligence. Based on the recent successes of deep learning,
512 especially the CNN feature representation and the LSTM with attention model,
513 the paper proposes the use of a hierarchical attention mechanism, considering
514 not only the global image features but also detected object features, with im-
515 proved results. A significant improvement over the current RNN-based MLE
516 training has also been demonstrated. Specifically, a GAN framework with RL
517 optimization for the image captioning task is proposed to generate more accurate
518 and high-quality captions. The discriminator is to evaluate the coherence and
519 consistency between the generated sentences and image content, thus providing
520 the rewards for optimization. The whole model follows a three-step training
521 strategy. Experiments analysis confirms the merits of the framework and key
522 contributors the improved performance. Comparable results with current state-
523 of-the-art methods are achieved using only greedy inference, which proves the

1
2
3
4
5
6
7
8
9 524 effectiveness of the training procedure.

10
11
12 525 **References**

13
14
15 526 **References**

- 16
17 527 [1] A. Krizhevsky, I. Sutskever, G. E. Hinton, Imagenet classification with deep
18
19 528 convolutional neural networks, in: NIPS, 2012.
- 20
21
22 529 [2] K. Simonyan, A. Zisserman, Very deep convolutional networks for large-
23
24 530 scale image recognition, in: ICLR, 2015.
- 25
26
27 531 [3] K. He, X. Zhang, S. Ren, J. Sun, Deep residual learning for image recogni-
28
29 532 tion, in: CVPR, 2016.
- 30
31 533 [4] S. Tang, Y. T. Zheng, Y. Wang, T. S. Chua, Sparse ensemble learning for
32
33 534 concept detection, IEEE Transactions on Multimedia 14 (1) (2012) 43–54.
- 34
35
36 535 [5] C. Kang, S. Xiang, S. Liao, C. Xu, C. Pan, Learning consistent feature
37
38 536 representation for cross-modal multimedia retrieval, IEEE Transactions on
39
40 537 Multimedia 17 (3) (2015) 370–381.
- 41
42 538 [6] S. Bu, Z. Liu, J. Han, J. Wu, R. Ji, Learning high-level feature by deep
43
44 539 belief networks for 3-d model retrieval and recognition, IEEE Transactions
45
46 540 on Multimedia 16 (8) (2014) 2154–2167.
- 47
48
49 541 [7] P. Liu, J. M. Guo, C. Y. Wu, D. Cai, Fusion of deep learning and com-
50
51 542 pressed domain features for content-based image retrieval, IEEE Transac-
52
53 543 tions on Image Processing 26 (12) (2017) 5706–5717.
- 54
55 544 [8] R. Girshick, J. Donahue, T. Darrell, J. Malik, Rich feature hierarchies for
56
57 545 accurate object detection and semantic segmentation, in: CVPR, 2014.

1
2
3
4
5
6
7
8
9
10
11
12
13
14
15
16
17
18
19
20
21
22
23
24
25
26
27
28
29
30
31
32
33
34
35
36
37
38
39
40
41
42
43
44
45
46
47
48
49
50
51
52
53
54
55
56
57
58
59
60
61
62
63
64
65

546 [9] R. Girshick, Fast r-cnn, in: ICCV, 2015.

547 [10] S. Ren, K. He, R. Girshick, J. Sun, Faster r-cnn: Towards real-time object
548 detection with region proposal networks, in: NIPS, 2015.

549 [11] G. Kulkarni, V. Premraj, V. Ordonez, S. Dhar, S. Li, Y. Choi, A. C. Berg,
550 T. L. Berg, Babytalk: Understanding and generating simple image descrip-
551 tions, *IEEE Transactions on Pattern Analysis and Machine Intelligence*
552 35 (12) (2013) 2891–2903.

553 [12] H. Fang, S. Gupta, F. Iandola, R. K. Srivastava, L. Deng, P. Dollár, J. Gao,
554 X. He, M. Mitchell, J. C. Platt, et al., From captions to visual concepts
555 and back, in: CVPR, 2015.

556 [13] A. Karpathy, L. Fei-Fei, Deep visual-semantic alignments for generating
557 image descriptions, in: CVPR, 2015.

558 [14] O. Vinyals, A. Toshev, S. Bengio, D. Erhan, Show and tell: A neural image
559 caption generator, in: CVPR, 2015.

560 [15] K. Cho, B. van Merriënboer, D. Bahdanau, Y. Bengio, On the properties
561 of neural machine translation: Encoder–decoder approaches, in: Proceed-
562 ings of SSST-8, Eighth Workshop on Syntax, Semantics and Structure in
563 Statistical Translation, 2014.

564 [16] K. Cho, A. Courville, Y. Bengio, Describing multimedia content using
565 attention-based encoder-decoder networks, *IEEE Transactions on Multi-
566 media* 17 (11) (2015) 1875–1886.

567 [17] D. Bahdanau, K. Cho, Y. Bengio, Neural machine translation by jointly
568 learning to align and translate, in: ICLR, 2015.

- 1
2
3
4
5
6
7
8
9
10
11
12
13
14
15
16
17
18
19
20
21
22
23
24
25
26
27
28
29
30
31
32
33
34
35
36
37
38
39
40
41
42
43
44
45
46
47
48
49
50
51
52
53
54
55
56
57
58
59
60
61
62
63
64
65
- 569 [18] K. Xu, J. Ba, R. Kiros, K. Cho, A. Courville, R. Salakhudinov, R. Zemel,
570 Y. Bengio, Show, attend and tell: Neural image caption generation with
571 visual attention, in: ICML, 2015.
- 572 [19] L. Li, S. Tang, Y. Zhang, L. Deng, Q. Tian, Gla: Global-local attention for
573 image description, IEEE Transactions on Multimedia PP (99) (2017) 1–1.
- 574 [20] S. Bengio, O. Vinyals, N. Jaitly, N. Shazeer, Scheduled sampling for se-
575 quence prediction with recurrent neural networks, in: NIPS, 2015.
- 576 [21] B. Dai, S. Fidler, R. Urtasun, D. Lin, Towards diverse and natural image
577 descriptions via a conditional gan, in: CVPR, 2017.
- 578 [22] I. Goodfellow, J. Pouget-Abadie, M. Mirza, B. Xu, D. Warde-Farley,
579 S. Ozair, A. Courville, Y. Bengio, Generative adversarial nets, in: NIPS,
580 2014.
- 581 [23] M. Mirza, S. Osindero, Conditional generative adversarial nets, arXiv
582 preprint arXiv:1411.1784.
- 583 [24] R. S. Sutton, A. G. Barto, Reinforcement learning: An introduction, Vol. 1,
584 MIT press Cambridge, 1998.
- 585 [25] L. Yu, W. Zhang, J. Wang, Y. Yu, Seqgan: Sequence generative adversarial
586 nets with policy gradient., in: AAAI, 2017.
- 587 [26] R. S. Sutton, D. A. McAllester, S. P. Singh, Y. Mansour, Policy gradient
588 methods for reinforcement learning with function approximation, in: NIPS,
589 2000.
- 590 [27] D. Silver, A. Huang, C. J. Maddison, A. Guez, L. Sifre, G. Van Den Driess-
591 che, J. Schrittwieser, I. Antonoglou, V. Panneershelvam, M. Lanctot, et al.,

1
2
3
4
5
6
7
8
9
10
11
12
13
14
15
16
17
18
19
20
21
22
23
24
25
26
27
28
29
30
31
32
33
34
35
36
37
38
39
40
41
42
43
44
45
46
47
48
49
50
51
52
53
54
55
56
57
58
59
60
61
62
63
64
65

592 Mastering the game of go with deep neural networks and tree search, *Nature*
593 529 (7587) (2016) 484–489.

594 [28] J. Mao, W. Xu, Y. Yang, J. Wang, Z. Huang, A. Yuille, Deep caption-
595 ing with multimodal recurrent neural networks (m-rnn), arXiv preprint
596 arXiv:1412.6632.

597 [29] X. Jia, E. Gavves, B. Fernando, T. Tuytelaars, Guiding long-short term
598 memory for image caption generation, arXiv preprint arXiv:1509.04942.

599 [30] J. Donahue, L. Anne Hendricks, S. Guadarrama, M. Rohrbach, S. Venugopalan,
600 K. Saenko, T. Darrell, Long-term recurrent convolutional net-
601 works for visual recognition and description, in: CVPR, 2015.

602 [31] K. Cho, B. Van Merriënboer, C. Gulcehre, D. Bahdanau, F. Bougares,
603 H. Schwenk, Y. Bengio, Learning phrase representations using rnn encoder-
604 decoder for statistical machine translation, arXiv preprint arXiv:1406.1078.

605 [32] V. Mnih, N. Heess, A. Graves, et al., Recurrent models of visual attention,
606 in: NIPS, 2014.

607 [33] J. Ba, V. Mnih, K. Kavukcuoglu, Multiple object recognition with visual
608 attention, arXiv preprint arXiv:1412.7755.

609 [34] L. Yao, A. Torabi, K. Cho, N. Ballas, C. Pal, H. Larochelle, A. Courville,
610 Describing videos by exploiting temporal structure, in: ICCV, 2015.

611 [35] Q. You, H. Jin, Z. Wang, C. Fang, J. Luo, Image captioning with semantic
612 attention, in: CVPR, 2016.

613 [36] T. Yao, Y. Pan, Y. Li, Z. Qiu, T. Mei, Boosting image captioning with
614 attributes, in: ICCV, 2017.

1
2
3
4
5
6
7
8
9
10
11
12
13
14
15
16
17
18
19
20
21
22
23
24
25
26
27
28
29
30
31
32
33
34
35
36
37
38
39
40
41
42
43
44
45
46
47
48
49
50
51
52
53
54
55
56
57
58
59
60
61
62
63
64
65

615 [37] L. Chen, H. Zhang, J. Xiao, L. Nie, J. Shao, W. Liu, T.-S. Chua, Sca-
616 cnn: Spatial and channel-wise attention in convolutional networks for image
617 captioning, in: CVPR, 2017.

618 [38] A. Goyal, N. R. Ke, A. Lamb, R. D. Hjelm, C. Pal, J. Pineau,
619 Y. Bengio, Actual: Actor-critic under adversarial learning, arXiv preprint
620 arXiv:1711.04755.

621 [39] I. Goodfellow, Nips 2016 tutorial: Generative adversarial networks, arXiv
622 preprint arXiv:1701.00160.

623 [40] K. Papineni, S. Roukos, T. Ward, W.-J. Zhu, Bleu: a method for automatic
624 evaluation of machine translation, in: ACL, 2002.

625 [41] A. Lavie, A. Agarwal, Meteor: An automatic metric for mt evaluation with
626 improved correlation with human judgments, in: EMNLP Workshop on
627 Statistical Machine Translation, 2005.

628 [42] C.-Y. Lin, E. Hovy, Automatic evaluation of summaries using n-gram co-
629 occurrence statistics, in: NAACL, 2003.

630 [43] M. Ranzato, S. Chopra, M. Auli, W. Zaremba, Sequence level training with
631 recurrent neural networks, in: ICLR, 2016.

632 [44] S. Liu, Z. Zhu, N. Ye, S. Guadarrama, K. Murphy, Improved image cap-
633 tioning via policy gradient optimization of spider, in: ICCV, 2017.

634 [45] P. Anderson, B. Fernando, M. Johnson, S. Gould, Spice: Semantic propo-
635 sitional image caption evaluation, in: ECCV, 2016.

636 [46] R. Vedantam, C. Lawrence Zitnick, D. Parikh, Cider: Consensus-based
637 image description evaluation, in: CVPR, 2015.

- 1
2
3
4
5
6
7
8
9 638 [47] D. Bahdanau, P. Brakel, K. Xu, A. Goyal, R. Lowe, J. Pineau, A. Courville,
10 Y. Bengio, An actor-critic algorithm for sequence prediction, in: ICLR,
11 639
12 2017.
13 640
- 14
15 641 [48] T. Salimans, I. Goodfellow, W. Zaremba, V. Cheung, A. Radford, X. Chen,
16 Improved techniques for training gans, in: NIPS, 2016.
17 642
- 18
19 643 [49] M. Arjovsky, S. Chintala, L. Bottou, Wasserstein gan, arXiv preprint
20 arXiv:1701.07875.
21 644
- 22
23 645 [50] E. Jang, S. Gu, B. Poole, Categorical reparameterization with gumbel-
24 softmax, arXiv preprint arXiv:1611.01144.
25 646
- 26
27 647 [51] C. J. Maddison, A. Mnih, Y. W. Teh, The concrete distribution:
28 A continuous relaxation of discrete random variables, arXiv preprint
29 648 arXiv:1611.00712.
30 649
- 31
32 650 [52] R. Shetty, M. Rohrbach, L. A. Hendricks, M. Fritz, B. Schiele, Speaking
33 the same language: Matching machine to human captions by adversarial
34 training, in: ICCV, 2017.
35 651
36 652
- 37
38 653 [53] M. J. Kusner, J. M. Hernández-Lobato, Gans for sequences of dis-
39 crete elements with the gumbel-softmax distribution, arXiv preprint
40 654 arXiv:1611.04051.
41 655
- 42
43 656 [54] L. Wu, Y. Xia, L. Zhao, F. Tian, T. Qin, J. Lai, T.-Y. Liu, Adversarial
44 neural machine translation, arXiv preprint arXiv:1704.06933.
45 657
- 46
47 658 [55] O. Russakovsky, J. Deng, H. Su, J. Krause, S. Satheesh, S. Ma, Z. Huang,
48 A. Karpathy, A. Khosla, M. Bernstein, et al., Imagenet large scale visual
49 659
50
51
52
53
54
55
56
57
58
59
60
61
62
63
64
65

1
2
3
4
5
6
7
8
9
10
11
12
13
14
15
16
17
18
19
20
21
22
23
24
25
26
27
28
29
30
31
32
33
34
35
36
37
38
39
40
41
42
43
44
45
46
47
48
49
50
51
52
53
54
55
56
57
58
59
60
61
62
63
64
65

660 recognition challenge, *International Journal of Computer Vision* 115 (3)
661 (2015) 211–252.

662 [56] S. Hochreiter, J. Schmidhuber, Long short-term memory, *Neural computa-*
663 *tion* 9 (8) (1997) 1735–1780.

664 [57] R. J. Williams, Simple statistical gradient-following algorithms for connec-
665 *tionist reinforcement learning*, *Machine learning* 8 (3-4) (1992) 229–256.

666 [58] T. Tieleman, G. Hinton, Lecture 6.5-rmsprop: Divide the gradient by a
667 *running average of its recent magnitude*, *COURSERA: Neural networks*
668 *for machine learning* 4 (2) (2012) 26–31.

669 [59] D. Kingma, J. Ba, Adam: A method for stochastic optimization, in: *ICLR*,
670 2015.

671 [60] P.-T. De Boer, D. P. Kroese, S. Mannor, R. Y. Rubinstein, A tutorial on
672 *the cross-entropy method*, *Annals of operations research* 134 (1) (2005)
673 19–67.

674 [61] T.-Y. Lin, M. Maire, S. Belongie, J. Hays, P. Perona, D. Ramanan,
675 P. Dollár, C. L. Zitnick, Microsoft coco: Common objects in context, in:
676 *ECCV*, 2014.

677 [62] Y. Jia, E. Shelhamer, J. Donahue, S. Karayev, J. Long, R. Girshick,
678 S. Guadarrama, T. Darrell, Caffe: Convolutional architecture for fast fea-
679 *ture embedding*, in: *ACMMM*, 2014.

680 [63] M. Abadi, A. Agarwal, P. Barham, E. Brevdo, Z. Chen, C. Citro, G. S.
681 *Corrado*, A. Davis, J. Dean, M. Devin, et al., *Tensorflow: Large-scale*

1
2
3
4
5
6
7
8
9
10
11
12
13
14
15
16
17
18
19
20
21
22
23
24
25
26
27
28
29
30
31
32
33
34
35
36
37
38
39
40
41
42
43
44
45
46
47
48
49
50
51
52
53
54
55
56
57
58
59
60
61
62
63
64
65

682 machine learning on heterogeneous distributed systems, arXiv preprint
683 arXiv:1603.04467.

684 [64] X. Chen, C. L. Zitnick, Mind’s eye: A recurrent visual representation for
685 image caption generation, in: CVPR, 2015.

686 [65] J. Aneja, A. Deshpande, A. G. Schwing, Convolutional image captioning,
687 in: CVPR, 2018.

688 [66] L. A. Hendricks, S. Venugopalan, M. Rohrbach, R. Mooney, K. Saenko,
689 T. Darrell, Deep compositional captioning: Describing novel object cate-
690 gories without paired training data, in: CVPR, 2016.

691 [67] Z. Ren, X. Wang, N. Zhang, X. Lv, L.-J. Li, Deep reinforcement learning-
692 based image captioning with embedding reward, in: CVPR, 2017.

693 [68] S. J. Rennie, E. Marcheret, Y. Mroueh, J. Ross, V. Goel, Self-critical se-
694 quence training for image captioning, in: CVPR, 2017.